

Transition from a hysteresis-like to an exchange-bias-like response of an uncompensated antiferromagnet

Martin Buchner,^{*} Bastian Henne, Verena Ney, and Andreas Ney
*Institut für Halbleiter- und Festkörperphysik, Johannes Kepler Universität,
 Altenberger Strasse 69, 4040 Linz, Austria*

 (Received 29 August 2018; revised manuscript received 6 December 2018; published 11 February 2019)

Highly Co-doped ZnO shows uncompensated antiferromagnetic order and a vertical exchange bias shift even in the absence of a ferromagnet. Therefore, it is an ideal model system to study the behavior of uncompensated antiferromagnetic moments, which play a crucial role in the description of conventional exchange bias. Temperature- and cooling-field-dependent magnetometry measurements provide further information on the compensated and uncompensated antiferromagnetic configurations in Co-doped ZnO, revealing that observed effects of both vertical exchange shift and open hysteresis stem from similar magnetic configurations. This transition is evidenced by the increase of the vertical exchange shift on the expense of the hysteresis opening by lowering the temperature.

DOI: [10.1103/PhysRevB.99.064409](https://doi.org/10.1103/PhysRevB.99.064409)

I. INTRODUCTION

In a system consisting of a ferromagnetic (FM) and an antiferromagnetic (AFM) layer, the exchange bias effect may be observed [1–4]. Below the Curie temperature (T_C) of the FM and the Néel temperature T_N of the AFM, an additional coupling of FM and AFM magnetic moments close to the interface leads to changes of the FM hysteresis. The coercivity H_c increases and the hysteresis loop shifts horizontally along the magnetic field axis, usually in opposite direction of the cooling field [5,6]. Higher magnetic fields are therefore needed to reverse the magnetization of the exchange-biased FM layer compared to the nonbiased one. This is used in technical applications to pin FM layers in a certain direction, for example, in magnetic recording heads [7]. Furthermore, exchange bias has been reported in nanoparticle-composite systems [8,9] and in rare cases also in the absence of a FM [10,11].

Initially, it was assumed that the interaction is confined to a single monolayer at the interface [12]. However, over the years more refined models [13–16] combined with experimental results [3,16–22] revealed that the coupling extends over several Ångströms across the interface and that the exchange bias field is dependent on various parameters like surface roughness [13], AFM domains [14], spin flop coupling [15], and the distribution of (pinned) uncompensated AFM moments [17,19–22]. It was predicted that if uncompensated AFM moments get pinned in an exchange bias system, they additionally shift the hysteresis vertically [22].

Furthermore, the AFM exhibits an increased orbital magnetic moment [23,24]. X-ray magnetic circular dichroism (XMCD) measurements on $\text{Zn}_{1-x}\text{Co}_x\text{O}$ (Co:ZnO) revealed that this increase in orbital moment is independent of a FM layer in proximity [25].

The uncompensated antiferromagnetism in wurtzite Co:ZnO originates from Co dopants substituting for Zn. Next cation neighbors of Co are AFM coupled [26], but due to the incomplete substitution of Zn with Co their magnetic moments are not fully compensated. When measuring a field cooled (FC) $M(H)$ curve of Co:ZnO at low temperatures, the curve is narrowly opened and shifted vertically on the magnetization axis, i.e., a field-imprinted magnetization is present. The low-temperature behavior of Co:ZnO is similar to the conventional exchange bias effect but in complete absence of FM layers and can be described by an empirical model [11] that couples uncompensated effective magnetic moments m_{eff} to fully compensated antiferromagnetic Co-O-Co... dopant structures, which are coupled by a AFM next-cation neighbor-exchange coupling of $J/k_B = 15 \pm 3$ K [26,27]. This is illustrated in the top left corner of Fig. 1 where uncompensated magnetic moments are depicted as red arrows while the compensated AFM structures are depicted as green spheres. It should be noted here that the illustration is a simplification. Since the Co doping is above the coalescence limit (which is 20% for Co:ZnO [28]), there exist connected Co paths throughout the whole sample. Therefore, the effective magnetic moment can be a complex arrangement of not fully compensated moments along the compensated structures. Furthermore, also the compensated parts occur in various forms, sizes, and shapes. However, in the model only the varying volume of the compensated dopant configurations is taken into account. As explained in Ref. [11], the volume of the compensated Co-O-Co... structure can magnetically block the m_{eff} , to which it is coupled, during a $M(H)$ cycle. Finally, the $M(T)$ curves in Ref. [29] do not show a characteristic cusp in the ZFC curve,

^{*}martin.buchner@jku.at

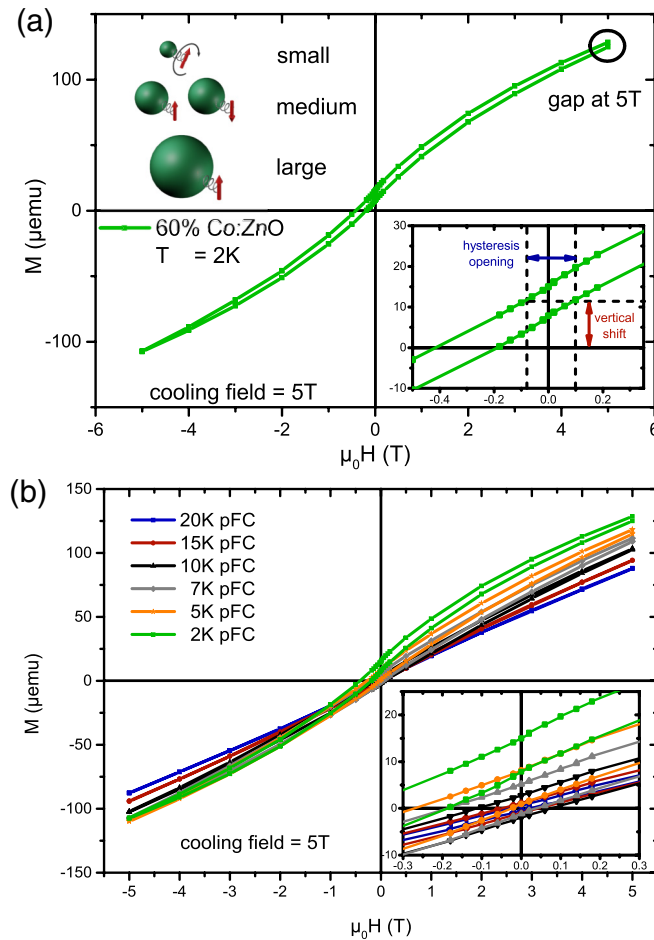


FIG. 1. Panel (a) shows the pFC magnetization curve of a 60% Co:ZnO film measured at 2 K. The red circle marks a gap between the starting and finishing value at 5 T, while the inset shows a loop shift and an open hysteresis. In the top left corner, a simple visualization of the size-dependent anisotropy model is depicted (more details in the text). For panel (b), the $M(H)$ curves are measured at different temperatures. The inset shows an enlargement around the zero-field region.

but a small bifurcation of the FC and ZFC measurement is visible. This bifurcation was assigned to spin-glass freezing in Ref. [30].

In this work, we expand the model introduced in Ref. [11] and study how temperature and cooling fields of different strengths influence the vertical exchange bias and thus the field-imprinted magnetization of Co:ZnO samples. Moreover, the magnetic properties of the Co ions are also changing with the overall Co-doping concentration. For example, by increasing the Co level, the magnetic moment per Co atom of $\mu = 3.4 \mu_B/\text{Co}$ for a single ion decreases [29,31]. The size of the hysteresis opening and the vertical shift of the Co:ZnO $M(H)$ curve depends on the Co-doping concentration. Therefore, for this work samples of different Co-doping concentrations with ample precharacterization [25,29,32] are studied as a function of temperature and cooling field, using superconducting quantum interference device (SQUID) magnetometry.

II. EXPERIMENTAL DETAILS

Co:ZnO films with Co concentrations of 30%, 50%, and 60% have been grown by reactive magnetron sputtering on c -plane Al_2O_3 substrates at a constant process gas pressure of 4×10^{-3} mbar, where the base pressure is below 2×10^{-9} mbar. The 30% and 50% samples have been sputtered using metallic targets of Co and Zn at a Ar : O₂ ratio of 10 : 1 standard cubic centimeter per minute (sccm), a sputter power of 20 W, and a substrate temperature of 450 °C (30%) and 294 °C (50%). These parameters yield an optimized crystalline quality [32]. The film containing 60% Co has been sputtered from a ZnO and Co₃O₄ ceramic composite target with a 3:2 ratio using only Ar as sputter gas, a sputter power of 30 W, and a substrate temperature of 525 °C [33]. All films have been grown with a nominal thickness of 200 nm. The optimized crystal structure utilizing those parameters was confirmed by x-ray diffraction (XRD) and x-ray linear and circular dichroism (XLD, XMCD) and published in earlier works [25,29].

Integral magnetization measurements were performed using a commercial SQUID magnetometer (Quantum Design, MPMS-XL5) in magnetic fields up to ± 5 T applied in the sample plane, which corresponds to the magnetic easy plane [11], due to the single-ion anisotropy of $D/k_B = 4 \pm 1$ K [26,29]. The magnetization curves are corrected for the diamagnetic background of the substrate obtained from high-field $M(H)$ data at 300 K [34] and care was taken to minimize the measurement artifacts described in Refs. [34–37]. Cooling-field-dependent measurements were conducted after cooling the films from room temperature, so well above T_N for all concentrations [29], to 2 K in a positive (plus field cooled, pFC) or negative (minus field cooled, mFC) external magnetic field of varying strength. To obtain the temperature-dependent behavior of hysteresis opening and vertical shift, the films were cooled in +5 T to different temperatures between 20 and 2 K, always heating up to 300 K in between two measurements.

III. EXPERIMENTAL RESULTS

Figure 1(a) shows a pFC magnetization curve of a 60% Co:ZnO film measured at 2 K. Similar to the results reported in Ref. [11] for 60% Co:ZnO, the magnetization curve is shifted upward to the positive magnetization direction with an open hysteresis in the entire field range. The inset demonstrates how vertical shift and hysteresis opening were extracted from the magnetization curve. Further, the magnetization does not return to its original starting value, resulting in a small gap between start and end points. This gap is attributed to frustrated spins in the system and vanishes by doing a second consecutive hysteresis. Therefore, it holds similarities to the training effect in conventional exchange-bias systems. Similar to Co:ZnO samples in Refs. [11,29,33], no saturation of the $M(H)$ curves is visible up to 5 T. From the XMCD(H) of Co:ZnO, it is known that even up to 17 T no saturation is visible for various Co concentrations [25,29,33], which is a clear indication of antiferromagnetic ordering. Furthermore, XLD and XMCD spectra of the studied samples exhibit no sign of metallic Co precipitates; cf. Refs. [25,29,33]. Note that it was shown in Ref. [29] that no vertical shift is present in

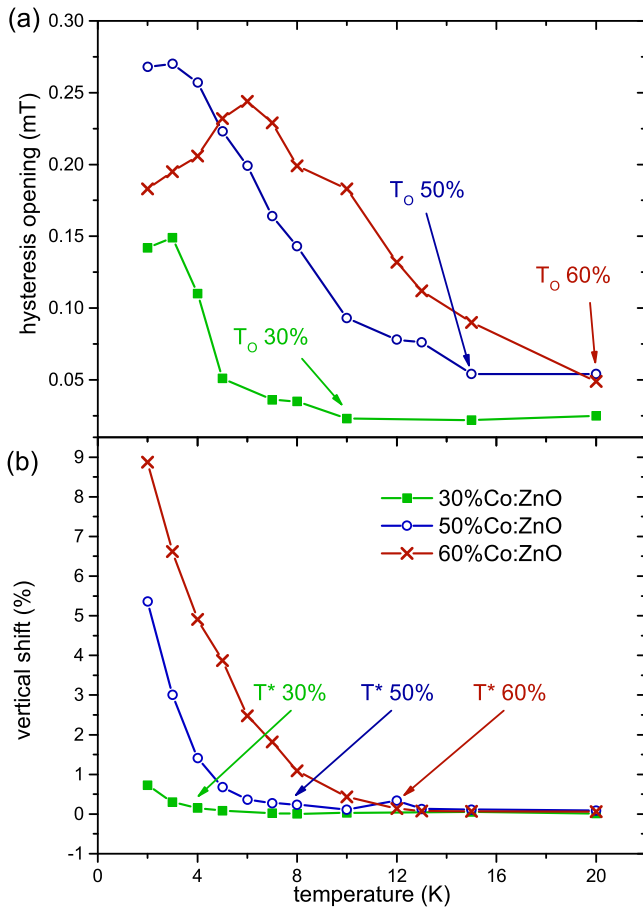


FIG. 2. In panel (a), the temperature dependence of the hysteresis opening for 30%, 50%, and 60% Co:ZnO obtained after plus field cooling in 5 T is shown. Panel (b) gives the corresponding temperature dependence of the vertical shift. From the measurements, onset temperatures for hysteresis opening T_0 and vertical shift T^* can be determined.

phase pure 20% Co:ZnO samples which in turn rules out any influence of the sapphire substrate on the findings presented here, since all samples were grown on sapphire from the same batch, which exhibits only a very weak paramagnetic contribution below 1% to the total magnetic signal.

Subsequent to the pFC process, $M(H)$ curves for different temperatures from 2 to 20 K have been recorded. As seen in Fig. 1(b), the hysteresis opening and vertical shift decrease when the temperature is increased. Above 20 K (T_N of 60% Co:ZnO [29]), the $M(H)$ curve is closed and no vertical shift is visible.

Figure 2 shows the temperature dependence of the hysteresis opening [Fig. 2(a)] and the vertical shift [Fig. 2(b)] for the three Co concentrations of 30% Co:ZnO (green squares), 50% Co:ZnO (open blue circles), and 60% Co:ZnO (red crosses). The vertical shift, extracted according to the definition given in the inset of Fig. 1(a), is given in percent of the magnetization at +5 T to account for different sample sizes and thus different sample volumes. All the measured raw data can be found in Ref. [38]. Similar to T_N [29], also the hysteresis opening and vertical shift are observed at higher temperatures for 60% Co:ZnO. The temperatures T^* , where first finite

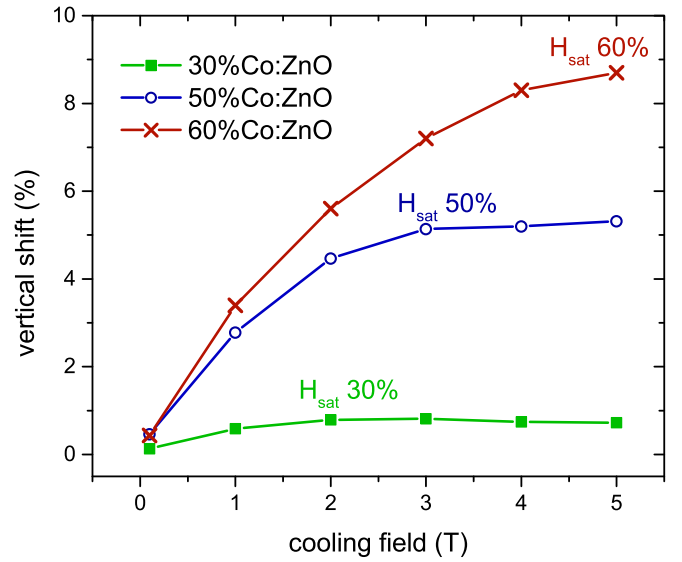


FIG. 3. Cooling-field dependence of the vertical exchange shift for the three different Co concentrations measured at 2 K.

shifts are observed, increase from 4 K for 30% Co:ZnO to roughly 12 K for 60% Co:ZnO. Likewise, the hysteresis onset temperatures T_0 increase from 10 to 20 K. Furthermore, the temperature dependence of the opening is different from the vertical shift. While the vertical shift is constantly increasing by lowering the temperature, the hysteresis opening reaches a maximum at around 3 K for the lower Co concentrations. In contrast, for 60% Co:ZnO, the hysteresis opening even starts to decrease again below 7 K.

In the model introduced in Ref. [11], the effective moment was taken as constant. To obtain more information on the uncompensated effective Co moments, a closer look at the influence of a magnetic field while cooling has to be taken. Therefore, $M(H)$ measurements were conducted at 2 K after the films were cooled in different magnetic fields. The results are shown in Fig. 3. For 30% Co:ZnO, a clear saturation of the vertical shift with a cooling field $H_{sat} \approx 2$ T is visible. For 50% Co:ZnO, H_{sat} is increased to 3 T. For 60% Co:ZnO, however, a nonzero slope remains up to 5 T, i.e. H_{sat} is about 5 T.

The magnetism of Co:ZnO does not only consist of uncompensated antiferromagnetic structures but additionally frustrated magnetic structures are present, as can be seen from the initial gap of the hysteresis in Fig. 1. In Fig. 4, the initial gap is shown as a function of cooling field and temperature (inset) for all three Co concentrations. In 60% Co:ZnO, large gaps are only observed below 10 K and with cooling fields above 3 T. In contrast, 30% Co:ZnO and 50% Co:ZnO show hardly any initial gap. Only at a cooling field of 5 T and at 2 K does the gap become significant. However, compared to 60% Co:ZnO, this gap is negligibly small. This shows that frustration becomes important only for the 60% Co-doped sample, so at the highest possible doping levels when more Co than Zn is present in the film.

IV. MODEL OF THE VERTICAL EXCHANGE BIAS

Following Ref. [11] the appearance of hysteresis opening and a vertical shift at 2 K can be described in a simple

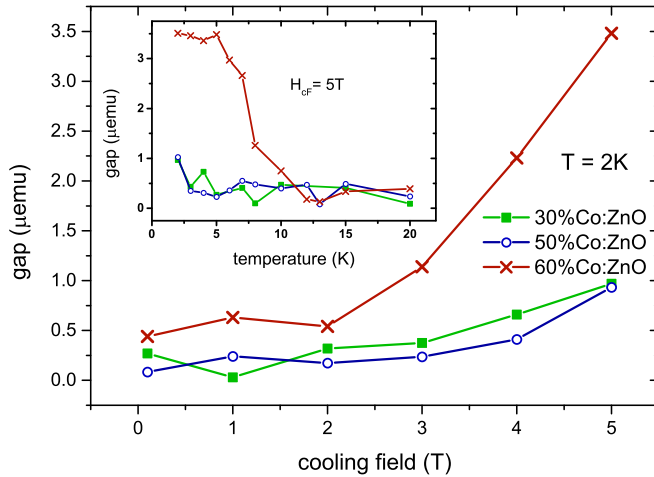


FIG. 4. The gap at +5 T is shown as a function of the cooling field for magnetization curves measured at 2 K. The temperature dependence is in the inset. Both measurements show a larger gap in the 60% Co:ZnO sample compared to 30% and 50% Co:ZnO.

Stoner-Wolfahrt-like approach. Three relevant energies determine the magnetic behavior of the Co moments: First, the Zeeman energy $E_Z = m_{\text{eff}}H$ of the uncompensated effective Co moments m_{eff} (red arrows in the top left corner of Fig. 1) in the external magnetic field during the $M(H)$ cycle. The maximum Zeeman energy corresponds to the highest possible magnetic field of 5 T for the SQUID magnetometer, so $E_Z^{\text{max}} = m_{\text{eff}} \times 5$ T. Second, the thermal energy $E_T = k_B T$ corresponds to the temperature at which the hysteresis is measured. Third, the size-dependent anisotropy energy E_A of compensated Co-O-Co... structures (represented by the green spheres in the top left corner of Fig. 1) are exchange coupled to the effective moment: $E_A \sim KV$, with anisotropy constant K and volume V of the Co-O-Co... structures. E_A is zero directly at T_N and increases by lowering the temperature, so at T_N the effective moments align according to the applied cooling field and can be blocked at lower temperatures by the increasing E_A . During a $M(H)$ cycle, the moments experience E_Z trying to align m_{eff} with H . To achieve parallel alignment, E_Z has to be higher than E_T . However, both energies oppose the blocking of m_{eff} induced by the anisotropy, so to really block m_{eff} against temperature and field, E_A of the compensated part has to be higher than the sum of E_Z and E_T .

In the following, we will distinguish between three size categories of compensated structures: small, medium, and large. This classification is determined from the behavior of effective moments, which are exchange coupled to the compensated parts, during the $M(H)$ cycle. Small structures align freely in the magnetic field (as indicated by the rotating arrow in Fig. 1), i.e., E_A is too small to block m_{eff} at the given E_T . Medium ones are blocked against temperature but with the additional E_Z they can be switched by the magnetic field and therefore cause the hysteresis opening (as indicated by the arrows for the medium structures in Fig. 1). Large structures are causing the vertical shift because their magnetic moment is blocked against temperature and magnetic field (as indicated by the fixed arrow in the inset of Fig. 1). We take this classification of Ref. [11] as starting point and extend

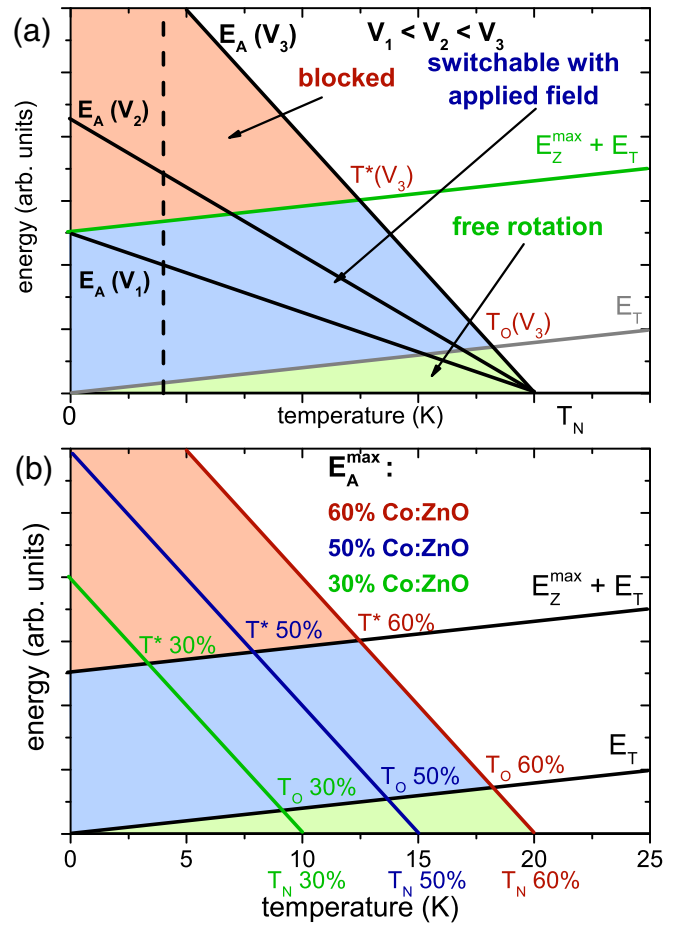


FIG. 5. The variation of anisotropy energy E_A of three different compensated Co-O-Co... structures is indicated as E_A of V_1 , V_2 , and V_3 , with V_3 marking the largest appearing structure. By increasing volume and thus anisotropy, the critical points for the transition from a free rotating effective moments (green area) to field switchable (blue area) or blocked (red area) increase in temperature. In panel (b), the model is adjusted for the different T_N for 30%, 50%, and 60% Co:ZnO.

it to model the temperature behavior of the system and in a second step also the Co concentration behavior. For the most simplistic approach of the compensated Co-O-Co... structures, E_A is assumed to increase linearly with decreasing temperature, starting from T_N . So $K(T) = -kT + K_0$, resulting in $E_A \sim (-kT + K_0)V$. Furthermore, the anisotropy constants k and K_0 are assumed to be uniform in every structure size, so that larger slopes in E_A correspond directly to a larger volume of the compensated structures.

All these assumptions for E_A lead to the temperature dependence of the system illustrated in Fig. 5(a). E_Z^{max} corresponds to the Zeeman energy at 5 T in the $M(H)$ cycle of the SQUID. The anisotropy is given for three different compensated Co-O-Co... structures of volumes $V_1 < V_2 < V_3$ with V_3 corresponding to the largest appearing structure, i.e., maximum E_A . Critical points for the temperature behavior are reached when E_A crosses either E_T or the sum of $E_T + E_Z$. As long as the anisotropy energy is smaller than the thermal energy, indicated as the light green area, the effective

moment of the structure can rotate freely (=small structures). When the anisotropy exceeds the thermal energy, the effective moment becomes blocked against thermal fluctuations. With the energy E_Z of the magnetic field, however, the moments can be switched and align parallel to the field, causing the open hysteresis (=medium structures). Up to E_Z^{\max} determined by the maximum magnetic field, the light blue area captures all the switchable structures, giving rise to the hysteresis opening. If E_A surpasses $E_T + E_Z$, the effective moment of a structure remains blocked across the entire field range up to the maximum E_Z (=large structures), indicated by the orange area. The determination if a structure of given volume is free, field-rotatable, or blocked at a given temperature can be done by going along a vertical line at that temperature looking for E_A of the right volume, as indicated with the black dashed line. By going along an anisotropy line, the characteristic points in temperature where the transitions happen can be determined. Going along the anisotropy energy for V_3 [$E_A(V_3)$] is an example: Close to T_N , the first characteristic point $T_O(V_3)$ is reached, marking the transition from free rotation to field-applied rotation and thus E_A exceeds E_T . By lowering the temperature, a second characteristic point $T^*(V_3)$ is reached when E_A exceeds $E_T + E_Z$. Below this temperature, the effective moment m_{eff} gets blocked. Effective moments coupled to structures with a volume of V_1 or lower undergo only one transition from free rotation to switchable but never become blocked. As the volume decreases, this transition point is lowered in temperature. Note that the situation of no more free moments is only hypothetically reached at 0 K.

As exemplarily shown in Fig. 5(b) for the largest structures V_3 , T_N increases with increasing Co concentration [29]. Consequently, also the transition temperatures T_O and T^* shift to higher temperatures. Note that Fig. 5(b) implies simplifications: On the one hand, we assume an identical slope of E_A , i.e., the same maximum volume and thus anisotropy occurring for all Co concentrations. On the other hand, we do not consider the actual abundance of small, medium, and large structures for a given Co concentration.

Two conclusions can be drawn from these simple assumptions of a linear increase of K with temperature. First, the hysteresis opening is visible at higher temperatures than the vertical shift, which should only be observable at temperatures well below T_N . Furthermore, T_O and T^* increase with the Co concentration. Second, by cooling down further, more moments get blocked. Every effective moment coupled to a compensated structure with a volume like V_2 and thus an anisotropy energy in between $E_A(V_3)$ and $E_A(V_1)$ starts contributing to the hysteresis opening close to T_N , but at lower temperatures they contribute to the vertical exchange shift, indicating stronger shifts on the expense of the hysteresis opening. A more complex model of the temperature dependence of K does not alter this behavior but only shifts the characteristic temperatures for the transitions from free to field switchable to blocked. Finally, it should be noted that switching a magnetic moment is a thermally activated process, resulting in an Arrhenius like switching behavior. So, the considerations above where energies are directly compared can only give a qualitative result for switching temperatures. In reality, the lines in Fig. 5 are smeared out and close to the crossing points time-dependent effects also come into play.

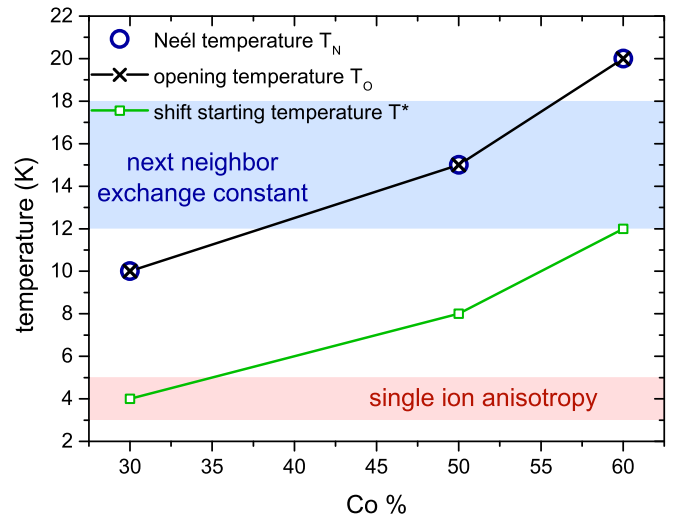


FIG. 6. A summary of the temperature dependence of hysteresis opening and vertical shift in Co:ZnO plotted over Co-doping level is given. For all Co concentrations, the hysteresis opening is in close vicinity to the T_N while the vertical shift only sets in at lower temperatures. Furthermore, single-ion anisotropy and exchange constant are shown within their error bars (see text) as shaded regions.

V. DISCUSSION

Figure 6 shows a summary of the temperature-dependent properties of the SQUID measurements. The Néel temperatures T_N as determined in $M(T)$ measurements [29] (open circles), the temperatures T_O at which the hysteresis opens (crosses), and the temperatures T^* where the loops start to shift (squares) are plotted versus Co concentration. Additionally, the quantities for single-ion anisotropy and the next neighbor exchange coupling constant are given as shaded areas covering their values within error bars ($D/k_B = 4 \pm 1$ K and $J/k_B = 15 \pm 3$ K), as reported in Refs. [26,27,29]. As predicted in the temperature-dependent model in Sec. IV, T_O and T^* increase with increasing Co content. A further accordance is that while the onset of the hysteresis opening T_O seems to follow the ordering temperature nicely, the vertical shift becomes nonzero only at temperatures below T_N . This is similar to the behavior in classical exchange-bias systems where the (horizontal) $M(H)$ loop shifts only appear at blocking temperatures T_B below the corresponding order temperature [39,40]. In conventional systems, the blocking temperature is assumed to be caused by different grain sizes and thicknesses of the AFM layers [1]. In Co:ZnO, however, as discussed in Sec. IV, the appearance of a vertical shift is determined by the blocking of effective moments. For a specific volume (and thus E_A) of the compensated Co-O-Co... part, m_{eff} is either field switchable or fully blocked, depending on the temperature. Following the assumptions of the temperature-dependent model, the fully blocked state is reached only at lower temperatures compared to the field-switchable state. Furthermore, looking at Fig. 2(a), it can be concluded that at 7 K a point in temperature is reached where the transition rate of moments becoming field switchable equals the rate of moments becoming blocked. Cooling below this point means more moments become blocked and thus the

vertical shift increases at the expense of the hysteresis opening. As indicated by the model, for 30% Co:ZnO and 50% Co:ZnO this characteristic point shifts to very low temperatures, so that the maximum barely is reached and no decrease can be observed. That the observed hysteresis opening and vertical shift are weaker for lower Co concentrations is expected, since a higher amount of Co in the film naturally leads to an increased probability of larger Co-O-Co-... structures. This does not necessarily mean that the volume per structure gets larger but that the abundance of large volume structures increases with the Co concentration. The higher abundance of larger volumes is evidenced further by the steeper onset of the hysteresis opening or the vertical shift with increasing Co content in the films. Additionally, below 5 K, the hysteresis opening of 50% Co:ZnO is wider than for 60% Co:ZnO, meaning at these temperatures 50% Co:ZnO has the highest amount of field-switchable structures.

In 30% Co:ZnO, the vertical shift becomes nonzero at temperatures corresponding to the single-ion anisotropy, indicated as light red region. However, by increasing the Co content, the shift increases and thus the imprinted magnetization is persistent up to temperatures which clearly exceed the single-ion anisotropy. Furthermore, the anisotropy decreases for higher Co-doping concentrations [29]. For 60% Co:ZnO, the temperature where the vertical shift is observed nearly reaches the next-neighbor exchange constant. This underlines that the vertical shift has its microscopic origin in the incomplete AFM order rather than in the single-ion anisotropy.

On the one hand, the degree of AFM compensation is increased at higher doping levels; this is verified by a decreasing effective magnetic moment per Co atom [29]. On the other hand, the higher doping level leads to a higher degree of magnetic frustration in the films [11]. To gain more information on m_{eff} from Figs. 3 and 4, a closer look at the cooldown process is taken. During the cooldown, the magnetic moments in Co:ZnO films are aligned in the direction of the applied magnetic field if their Zeeman energy exceeds the thermal energy. At T_N , the majority of Co dopants couples antiferromagnetically and only a fraction of not antiferromagnetically compensated Co moments m_{eff} remain. Following the assumptions before, these remaining moments stay aligned as long as the compensated part to which they are connected exhibits a sufficient anisotropy (the large structures) so that they contribute to vertical shift in the $M(H)$ curve. Thus, the vertical shift can be understood as sum over the m_{eff} coupled to large structures. Similar, the hysteresis stems from the m_{eff} of the medium structures. Since the size of the effective Co moments depends on the fraction of uncompensated to compensated Co moments in the film, it stays unchanged during the $M(H)$ cycle. Thus, the Zeeman energy close to T_N can only be altered by applying different magnetic fields.

Four conclusions can be drawn:

(1) Similar to the temperature dependence, also with cooling field it is clearly visible that samples with higher doping concentration exhibit larger vertical shifts. So again it can be concluded that the abundance of large compensated Co-O-Co-... structures is highest in 60% Co:ZnO.

(2) The Zeeman energy needed to align a moment is constant at the given T_N , so when stronger magnetic fields are needed for the shift to reach a stable (saturated) value it

means smaller magnetic moments are aligned. The saturation fields in Fig. 3 are roughly $H_{\text{sat}}(30\%) \sim 2$ T for 30% Co:ZnO, $H_{\text{sat}}(50\%) \sim 3$ T for 50% Co:ZnO, and $H_{\text{sat}}(60\%) \sim 5$ T for 60% Co:ZnO. From the different H_{sat} , a ratio of the m_{eff} in the films can be calculated. For example, the ratio for 50% Co:ZnO and 60% Co:ZnO is 0.6, similar to the ratio of their overall moments (so the sum over all m_{eff} divided by the number of Co atoms) of $0.25 \mu_B/\text{Co}$ (50%) and $0.15 \mu_B/\text{Co}$ (60%) determined from XMCD measurements [29]. In the same way, also the ratio of overall moments between 30–50% and 30–60% are matched, so the smallest magnetic moments contributing to the vertical shift are indeed related with the resulting Co moment per atom.

(3) The curvature of the cooling field dependence in Fig. 3 indicates that the films contain a distribution of uncompensated effective moments of different magnitudes. If there would be only one distinct moment, the cooling field dependence should be just a step function. As the Co content increases, the degree of compensation and the abundance of antiferromagnetically compensated structures of larger volume increases. Together with the conclusions of (2), it can be estimated that roughly one out of 23 Co moments is not compensated for the largest appearing structures in 60% Co:ZnO (calculated from the single Co moment of $3.4 \mu_B$, and the reduced effective moment of $0.15 \mu_B/\text{Co}$).

(4) Since Co:ZnO has the wurtzite crystal structure of ZnO, i.e., tetrahedral coordination, the effective moments contributing to the imprinted magnetization are not only uncompensated but a part of them is also magnetically frustrated. One consequence of this frustration is the appearance of a gap at 5 T in the SQUID measurements, as shown in Fig. 4. As already described in more detail in Ref. [11], the gap vanishes in a second consecutive cycle; however, the overall imprinted magnetization, i.e., the loop shift, is unchanged and can therefore be considered as loss of m_{eff} of the medium structures and thus as increase in antiferromagnetic compensation. From the conclusion above, it is clear that m_{eff} depends not on one single Co moment but on the amount of not fully compensated Co moments along a Co-O-Co-... structure. If the degree of antiferromagnetically compensated structures is increasing, the average distance between two uncompensated moments should increase as well, leading to a decrease in coupling strength. During the cooldown with applied magnetic field, E_Z is sufficient only at low temperatures to align two distant moments parallel in a weakly coupled frustrated state. During the $M(H)$ cycle when a magnetic field in opposite direction is applied, the distant moments can reorder and partially lose their parallel alignment.

VI. CONCLUSION

The vertical exchange bias in Co:ZnO has been studied over a wide doping range above the coalescence limit. The resulting dependencies on Co concentration, temperature, and cooling field were used to expand the model introduced in Ref. [11]. The behavior of compensated Co-O-Co-... structures while running a $M(H)$ cycle is used to define regions for medium-sized configurations (causing the hysteresis opening) and large structures (causing the vertical shift). The findings demonstrate that whether a structure belongs to the medium

or large category depends on temperature. By cooling down, structures which were originally contributing to the opening of the hysteresis start to contribute to the vertical shift, i.e., they go from the field switchable to the fully blocked state. For a Co concentration of 30%, this transition is barely observable and only the higher Co concentrations have a sufficient abundance of large Co-O-Co... configurations. Especially in 60% Co:ZnO, this transition is evidenced by the increase of the vertical exchange shift on the expense of the hysteresis opening. The observed dependence of the vertical exchange shift and the hysteresis opening in terms of temperature, cooling field, and Co concentration makes Co:ZnO an ideal model for uncompensated AFM systems. In turn, the Stoner-Wolfahrt-like model can consistently explain the microscopic

origin of the presence of a hysteresis and vertical exchange bias effect only based on simple assumptions for temperature and volume for the anisotropy of dopant configurations in uncompensated AFMs.

All the measured raw data can be found in the repository in Ref. [38].

ACKNOWLEDGMENTS

The authors gratefully acknowledge funding by the Austrian Science Fund (FWF) Projects No. P26164-N20 and No. ORD49-VO.

-
- [1] J. Nogués and I. K. Schuller, *J. Magn. Magn. Mater.* **192**, 203 (1999).
- [2] J. Nogués, C. Leighton, and I. K. Schuller, *Phys. Rev. B* **61**, 1315 (2000).
- [3] H. Ohldag, A. Scholl, F. Nolting, S. Anders, F. U. Hillebrecht, and J. Stöhr, *Phys. Rev. Lett.* **86**, 2878 (2001).
- [4] R. Rana, P. Pandey, R. P. Singh, and D. S. Rana, *Sci. Rep.* **4**, 4138 (2014).
- [5] W. P. Meiklejohn and C. P. Bean, *Phys. Rev.* **102**, 1413 (1956).
- [6] M. Gibert, P. Zubko, R. Scherwitzl, J. Íñiguez, and J.-M. Triscone, *Nat. Mater.* **11**, 195 (2012).
- [7] B. Dieny, V. S. Speriosu, S. S. P. Parkin, B. A. Gurney, D. R. Wilhoit, and D. Mauri, *Phys. Rev. B* **43**, 1297 (1991).
- [8] A. N. Dobrynin, D. N. Ievlev, K. Temst, P. Lievens, J. Margueritat, J. Gonzalo, C. N. Afonso, S. Q. Zhou, A. Van-tomme, E. Piscopiello, and G. Van Tendeloo, *Appl. Phys. Lett.* **87**, 012501 (2005).
- [9] X. Sun, N. F. Huls, A. Sigdel, and S. Sun, *Nano Lett.* **12**, 246 (2012).
- [10] R. H. Kodama, S. A. Makhlof, and A. E. Berkowitz, *Phys. Rev. Lett.* **79**, 1393 (1997).
- [11] B. Henne, V. Ney, M. de Souza, and A. Ney, *Phys. Rev. B* **93**, 144406 (2016).
- [12] W. H. Meiklejohn and C. P. Bean, *Phys. Rev.* **105**, 904 (1957).
- [13] A. P. Malozemoff, *Phys. Rev. B* **35**, 3679 (1987).
- [14] D. Mauri, H. C. Siegmann, P. S. Bagus, and E. Kay, *J. Appl. Phys.* **62**, 3047 (1987).
- [15] N. C. Koon, *Phys. Rev. Lett.* **78**, 4865 (1997).
- [16] M. R. Fitzsimmons, B. J. Kirby, S. Roy, Z.-P. Li, Igor V. Roshchin, S. K. Sinha, and Ivan K. Schuller, *Phys. Rev. B* **75**, 214412 (2007).
- [17] F. Nolting, A. Scholl, J. Stöhr, J. W. Seo, J. Fompeyrine, H. Siegwart, J.-P. Locquet, S. Anders, J. Lüning, E. E. Fullerton, M. F. Toney, M. R. Scheinfein, and H. A. Padmore, *Nature (London)* **405**, 767 (2000).
- [18] S. Brück, Gisela Schütz, E. Goering, X. Ji, and K. M. Krishnan, *Phys. Rev. Lett.* **101**, 126402 (2008).
- [19] E. Blackburn, C. Sanchez-Hanke, S. Roy, D. J. Smith, J.-I. Hong, K. T. Chan, A. E. Berkowitz, and S. K. Sinha, *Phys. Rev. B* **78**, 180408 (2008).
- [20] W. J. Antel Jr., F. Perjeru, and G. R. Harp, *Phys. Rev. Lett.* **83**, 1439 (1999).
- [21] I. Schmid, M. A. Marioni, P. Kappenberger, S. Romer, M. Parlinska-Wojtan, H. J. Hug, O. Hellwig, M. J. Carey, and E. E. Fullerton, *Phys. Rev. Lett.* **105**, 197201 (2010).
- [22] H. Ohldag, A. Scholl, F. Nolting, E. Arenholz, S. Maat, A. T. Young, M. Carey, and J. Stöhr, *Phys. Rev. Lett.* **91**, 017203 (2003).
- [23] D. Schmitz, E. Schierle, N. Darowski, H. Maletta, E. Weschke, and M. Gruyters, *Phys. Rev. B* **81**, 224422 (2010).
- [24] P. Audehm, M. Schmidt, S. Brück, T. Tietze, J. Gräfe, S. Macke, G. Schütz, and E. Goering, *Sci. Rep.* **6**, 25517 (2016).
- [25] M. Buchner, B. Henne, V. Ney, J. Lumetzberger, F. Wilhelm, A. Rogalev, A. Hen, and A. Ney, *J. Appl. Phys.* **123**, 203905 (2018).
- [26] A. Ney, V. Ney, F. Wilhelm, A. Rogalev, and K. Usadel, *Phys. Rev. B* **85**, 245202 (2012).
- [27] T. Chanier, M. Sargolzaei, I. Opahle, R. Hayn, and K. Koepf, *Phys. Rev. B* **73**, 134418 (2006).
- [28] C. Lorenz, R. May, and R. M. Ziff, *J. Stat. Phys.* **98**, 961 (2000).
- [29] V. Ney, B. Henne, J. Lumetzberger, F. Wilhelm, K. Ollefs, A. Rogalev, A. Kovacs, M. Kieschnick, and A. Ney, *Phys. Rev. B* **94**, 224405 (2016).
- [30] M. Sawicki, E. Guziejewicz, M. I. Łukasiewicz, O. Proselkov, I. A. Kowalik, W. Lisowski, P. Dłuzewski, A. Wittlin, M. Jaworski, A. Wolska, W. Paszkowicz, R. Jakiela, B. S. Witkowski, L. Wachnicki, M. T. Klepka, F. J. Luque, D. Arvanitis, J. W. Sobczak, M. Krawczyk, A. Jablonski, W. Stefanowicz, D. Szentkiel, M. Godlewski, and T. Dietl, *Phys. Rev. B* **88**, 085204 (2013).
- [31] P. Sati, R. Hayn, R. Kuzian, S. Régnier, S. Schäfer, A. Stepanov, C. Morhain, C. Deparis, M. Lügt, M. Goiran, and Z. Golacki, *Phys. Rev. Lett.* **96**, 017203 (2006).
- [32] B. Henne, V. Ney, J. Lumetzberger, K. Ollefs, F. Wilhelm, A. Rogalev, and A. Ney, *Phys. Rev. B* **95**, 054406 (2017).
- [33] B. Henne, V. Ney, K. Ollefs, F. Wilhelm, A. Rogalev, and A. Ney, *Sci. Rep.* **5**, 16863 (2015).
- [34] M. Sawicki, W. Stefanowicz, and A. Ney, *Semicond. Sci. Technol.* **26**, 064006 (2011).
- [35] A. Ney, T. Kammermeier, V. Ney, K. Ollefs, and S. Ye, *J. Magn. Magn. Mater.* **320**, 3341 (2008).
- [36] A. Ney, *Semicond. Sci. Technol.* **26**, 064010 (2011).

- [37] M. Buchner, K. Höfler, B. Henne, V. Ney, and A. Ney, *J. Appl. Phys.* **124**, 161101 (2018).
- [38] Data repository for Johannes Kepler University Linz (Magnetic Oxides Group) at <http://doi.org/10.17616/R3C78N>; search tag: BHN19.
- [39] D. Lederman, C. A. Ramos, V. Jaccarion, and J. L. Cardy, *Phys. Rev. B* **48**, 8365 (1993).
- [40] P. J. van der Zaag, A. R. Ball, L. F. Feiner, R. M. Wolf, and P. A. A. van der Heijden, *J. Appl. Phys.* **79**, 5103 (1996).